MATERIALS CHEMISTRY FRONTIERS

CHINESE CHEMICAL SOCIETY

ROYAL SOCIETY OF CHEMISTRY

RESEARCH ARTICLE

View Article Online
View Journal | View Issue

Cite this: *Mater. Chem. Front.*, 2020, **4**, 3594

An oxygen heterocycle-fused fluorene based non-fullerene acceptor for high efficiency organic solar cells†

Xin Ke,‡ Lingxian Meng,‡ Xiangjian Wan, Yanna Sun, Ziqi Guo, Simin Wu, Hongtao Zhang, Chenxi Li and Yongsheng Chen *

Received 7th May 2020,
Accepted 25th May 2020

DOI: 10.1039/d0qm00287a

rsc.li/frontiers-materials

A new acceptor–donor–acceptor (A–D–A) small molecule acceptor, named FCO-2F, is designed and synthesized based on the previous acceptor F-H. By inserting an oxygen atom into the backbone of F-H and fluorination on the end group, FCO-2F shows a much red-shifted absorption compared with F-H, and also a wider absorption up to 830 nm. Using polymer PM6 as the donor, the organic solar cell (OSC) devices based on FCO-2F offer a power conversion efficiency (PCE) of 13.36%, with a much improved short circuit current (J_{sc}) of 20.90 mA cm^{-2}.

Introduction

Organic solar cells (OSCs) have continuingly received increasing attention in recent years, owing to their advantages of low cost, light weight and flexibility.[1–3] Presently, the power conversion efficiencies (PCEs) of OSCs based on non-fullerene acceptors have reached impressive values of 16–17%.[4–18] Most of the successful non-fullerene acceptors have an acceptor–donor–acceptor (A–D–A) structure,[19–27] which has some intrinsic advantages including finely tunable energy levels, absorption and charge mobilities.[28,29] Although impressively high PCEs have been achieved, the performance of OSCs still lags behind that of inorganic solar cells such as silicon or perovskite cells.[30,31] But many theoretical studies have indicated that there is still large room to further enhance the performance of OSCs,[32] and one of the reasons is the wide chemical structure versatility of organic materials.

It is intuitive to have as wide and efficient light absorption as possible for the active materials before considering other factors. Indeed, great effort has been made to broaden the absorption spectra of active materials,[33–35] aiming to improve the short circuit current (J_{sc}) of OSCs for overall high performance. One of the features for the A–D–A type of molecules is that their highest occupied molecular orbital (HOMO) and lowest unoccupied molecular orbital (LUMO) are mainly decided by their corresponding central "D" and "A" units/groups.[36] This offers very convenient access to tune their HOMO/LUMO and absorption by modifying the central "D" unit and/or the end group "A" unit, either individually or together. In addition, the central "D" unit also plays an important role for forming suitable molecular packing and morphology. There are several effective methods applied to modify the donor D unit to achieve red-shifted absorption, such as extending the conjugation length,[24,25,33,37–44] changing the π bridge blocks,[45–49] and inserting oxygen into the backbone.[35,50–53] Among them, the method of inserting oxygen into the backbone could tune the HOMO energy level and give a further extended spectral response in the near-infrared region,[54] together with a fine-tuned intermolecular interaction for possible morphology optimization.[52,55] In most cases, this approach usually offers an increased J_{sc} and thus an improved PCE. In addition, great efforts have also been devoted to exploring new end groups, with the purpose of fine-tuning the "A" unit and LUMO.[56–61] Nowadays, halogen substitution on the widely used indanone end group (INCN)[62,63] has been intensively applied to adjust the LUMOs for a red-shifted absorption.[22,24,38,64,65]

In our previous work, we have designed an acceptor named FDICTF (F-H),[66] with a PCE of 10.06% when combined with the donor PBDB-T. The absorption onset of F-H is 760 nm, clearly too low for a high performance OPV material based on the theoretical works.[16,67] As discussed above, inserting oxygen into the backbone would cause a red-shifted absorption to obtain high J_{sc}. With these in mind, we design and synthesize FCO-2F with oxygen inserted in the backbone and a difluoro substituted end group (Fig. 1). Indeed, FCO-2F has a red-shifted absorption, with an absorption onset of 830 nm. Using PM6 as the donor, the OSC devices based on PM6:FCO-2F exhibit a PCE of 13.36%, with a J_{sc} of 20.90 mA cm^{-2}, much higher than F-H (PCE of 10.06% and J_{sc} of 15.81 mA cm^{-2}).[66]

State Key Laboratory and Institute of Elemento-Organic Chemistry, The Centre of Nanoscale Science and Technology and Key Laboratory of Functional Polymer Materials, Renewable Energy Conversion and Storage Center (RECAST), College of Chemistry, Nankai University, Tianjin, 300071, China.
E-mail: yschen99@nankai.edu.cn

† Electronic supplementary information (ESI) available. See DOI: 10.1039/d0qm00287a

‡ X. K. and L. M. contributed equally.

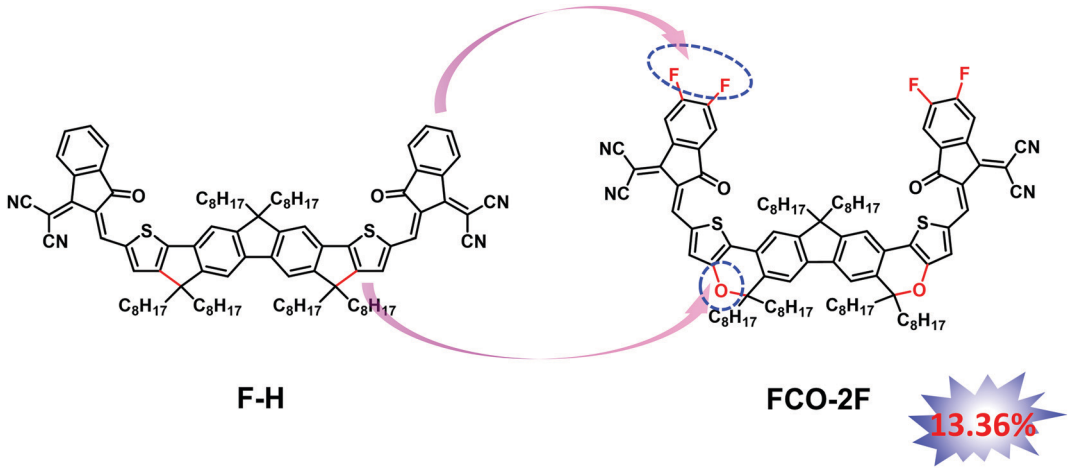

Fig. 1 Chemical structures of FCO-2F and F-H.

Results and discussion

The synthetic route of FCO-2F is shown in Scheme 1. The detailed procedures and characterization are summarized in the ESI.† This new molecule exhibits good solubility in common organic solvents, such as dichloromethane, chloroform and chlorobenzene. From the thermogravimetric analysis (TGA) curve in Fig. S1 (ESI†), the decomposition temperature (T_d) with 5% weight loss of FCO-2F is 307 °C, indicating its good thermal stability.

Theoretical calculation was carried out using density functional theory (DFT) at the B3LYP/6-31G* level to study its chemical geometry and molecular frontier orbitals. FCO-2F presents a nearly flat conformation similar to F-H (Fig. 2), indicating that the introduction of oxygen atoms into the backbone almost has no influence on the chemical geometry of the molecular backbone. The theoretically calculated HOMO/LUMO results of FCO-2F are −5.50/−3.48 eV. Compared with the theoretically calculated HOMO/LUMO results of F-H (−5.56/−3.30 eV),[61] the up-shifted HOMO level of FCO-2F is caused by the improvement of electron donating ability of the central core, while the down-shifted LUMO level is due to the difluoro substituted end group. These calculated results from DFT are in accordance with the experimental data discussed below.

As shown in Fig. 3a, in chloroform solution, FCO-2F has a clear red-shifted maximum absorption peak at 703 nm compared with that (665 nm) of F-H. Compared with the solution spectrum, the as-cast film of FCO-2F displays a significant red-shift of 53 nm with the maximum absorption peak at 756 nm and also a wide absorption range from 550 to 850 nm. This indicates that a more ordered aggregation is formed in the film. After thermal annealing (TA), the absorption peak of the FCO-2F film shows again an 18 nm red-shifted absorption with the absorption peak located at 774 nm. Furthermore, its absorption onset moves down to 830 nm, achieving a broader absorption spectrum than that of F-H (760 nm).

The energy levels of FCO-2F were measured by electrochemical cyclic voltammetry measurements in dichloromethane solution (Fig. S2, ESI†). The HOMO/LUMO levels for FCO-2F were estimated to be −5.37 and −3.78 eV, respectively. Compared with that (−5.43/−3.71 eV) of F-H,[66] the HOMO level of FCO-2F is up shifted and the LUMO level is down shifted, which results in a narrower bandgap as expected. These results are consistent with the calculated results discussed above.

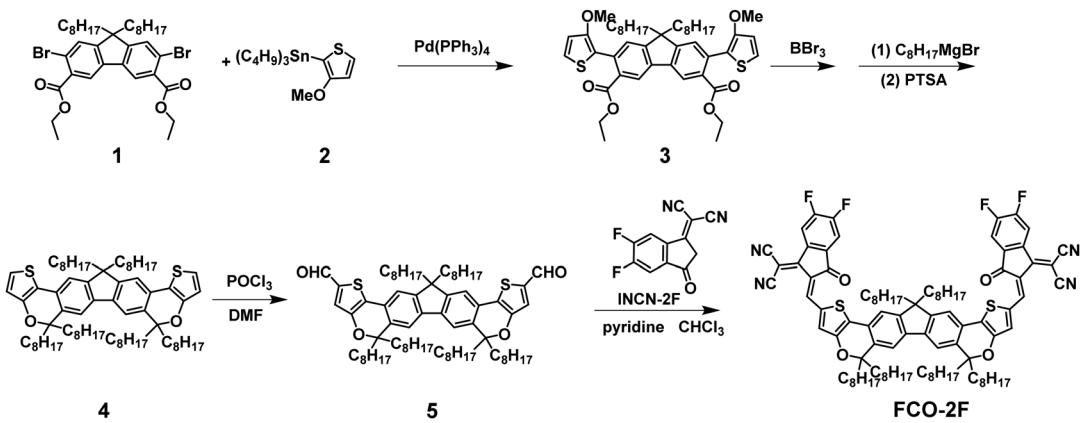

Scheme 1 Synthetic route of FCO-2F.

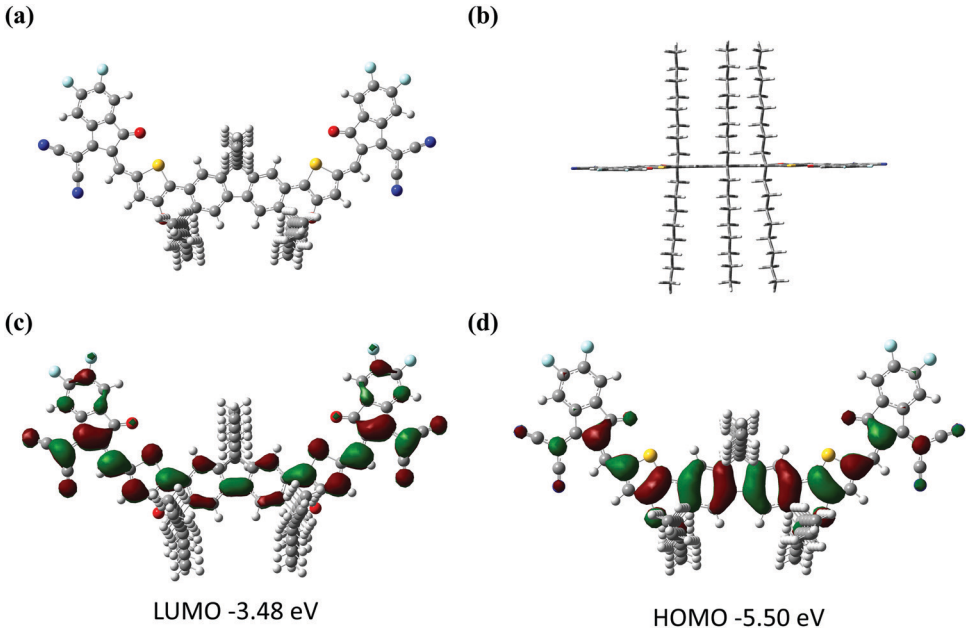

Fig. 2 The optimized geometries for FCO-2F from (a) top view and (b) side view. (c and d) Theoretical density distribution for the frontier molecular orbits of FCO-2F. All calculations were carried out using Gaussian 16.[68]

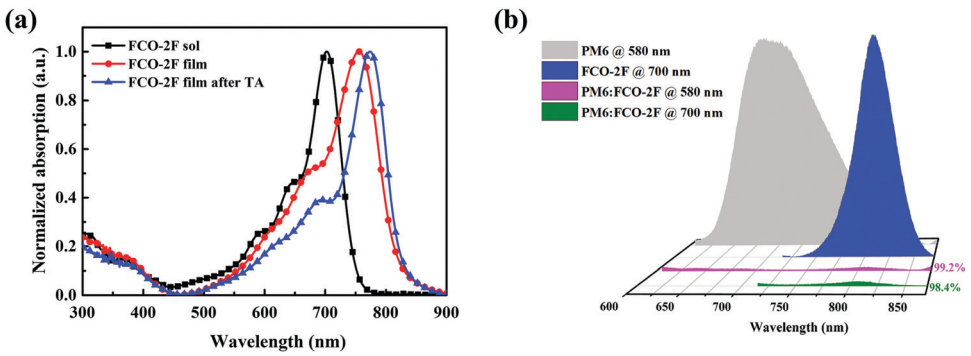

Fig. 3 (a) Normalized absorption spectra of FCO-2F in chloroform solution, its as-cast film and TA annealed film. (b) PL spectra of pure PM6, FCO-2F and the PM6:FCO-2F blend.

To evaluate the exciton dissociation efficiencies in the blend film, photoluminescence (PL) quenching tests of the pure films and blend film were measured (Fig. 3b). When excited at a wavelength of 580 nm, the PL emission peak of PM6 appears in the range of 650–850 nm. For the blend film of PM6:FCO-2F, the emission was quenched by 99.2%. When excited at a wavelength of 700 nm, the emission peak of FCO-2F was in the range of 750–850 nm. For the blend film, the emission was effectively fluorescence quenched by 98.4%. These results imply that efficient charge transfer could happen between PM6 and FCO-2F.

To assess the photovoltaic properties of FCO-2F, OSC devices were fabricated with an inverted device structure of indium tin oxide (ITO)/ZnO/PFN-Br/active layer/MoO_x/Ag. In consideration of the matched energy levels and complementary absorption with the acceptor, polymer PM6 was selected as the donor. The detailed results for device optimization are provided in the ESI† (Tables S1 and S2). The optimized photovoltaic parameters of FCO-2F together with those for F-H as a comparison are summarized in Table 1, and the corresponding *J–V* characteristics are shown in Fig. 4a. With the optimal weight ratio of donor and acceptor of 1 : 1, the devices based on PM6:FCO-2F with thermal annealing (TA) at 120 °C for 10 min show a PCE of 13.36%, with a high J_{sc} of 20.90 mA cm^{-2} and FF of 72.3%.

The external quantum efficiency (EQE) is measured and shown in Fig. 4b. The devices based on PM6:FCO-2F can reach a maximum EQE value of 85% and show a broader photo-to-current response range of 300–830 nm than that of F-H. The integrated current density for the FCO-2F device is 20.33 mA cm^{-2}, which is in good agreement with the J_{sc} values in the *J–V* measurement and a deviation of within 5%.

The charge generation and recombination behavior in the optimal PM6:FCO-2F based device were investigated. The photocurrent (J_{ph}) *versus* the effective applied voltage (V_{eff})

Table 1 Optimal device parameters of the FCO-2F based and F-H based devices under the illumination of AM 1.5G (100 mW cm^{-2})

BHJ layer	V_{oc} [V]	J_{sc} [mA cm^{-2}]	FF [%]	PCE[a] [%]
PM6:FCO-2F	0.884	20.90	72.3	13.36 (13.14)
PBDB-T:F-H[b]	0.940	15.81	66.0	10.06 (9.81)

[a] The average PCE was obtained from 10 devices, and the average results are provided in parentheses. [b] Data are obtained from ref. 66.

curve is shown in Fig. 4c. When V_{eff} reaches ~2 V, the J_{ph} value reaches saturation (J_{sat}), indicating that charge recombination is minimized at higher voltage. The value of J_{ph}/J_{sat} could reflect the exciton dissociation probability in the device.[69] Under the conditions of short circuit, the J_{ph}/J_{sat} ratio for the FCO-2F based device is 96.2%, implying that the high exciton dissociation and charge collection have high efficiencies and also consistent with the high FF. The light-intensity (P) dependence of J_{sc} was also measured to further study the charge recombination properties in the device using the power-law equation $J_{sc} \propto P^{\alpha}$ (Fig. 4d). The high α value of 0.929 for the device PM6:FCO-2F indicates that the bimolecular recombination that occurred in the optimal device is very weak.

The charge mobility of the blend film was measured by the space-charge-limited current (SCLC) method (Fig. S3, ESI†). The PM6:FCO-2F photoactive layer shows a hole mobility of 3.26×10^{-4} cm^{-2} V^{-1} s^{-1} and an electron mobility of 1.37×10^{-4} cm^{-2} V^{-1} s^{-1}, both are higher than those of the F-H based device (3.37×10^{-5}/2.40×10^{-5} cm^{-2} V^{-1} s^{-1}).[70]

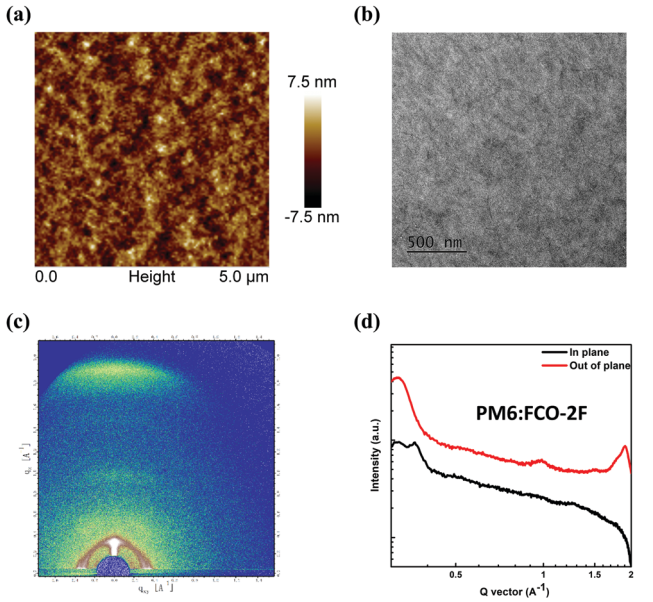

Fig. 5 (a) AFM and (b) TEM images of the PM6:FCO-2F blend film. (c) GIWAXS pattern for the PM6:FCO-2F blend. (d) In-plane and out-of-plane line cuts of the corresponding GIWAXS pattern.

The atomic force microscopy (AFM) and transmission electron microscopy (TEM) measurements were taken to study the morphologies of a PM6:FCO-2F blend film. As shown in the AFM image in Fig. 5a, the PM6:FCO-2F film shows good

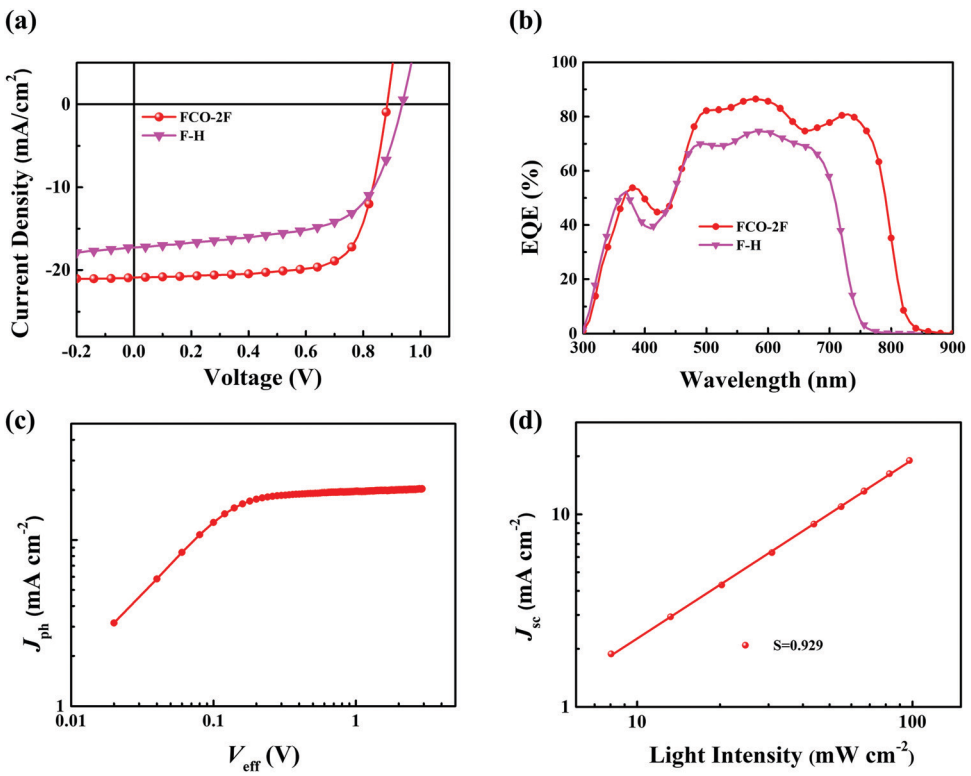

Fig. 4 (a) Optimal current density–voltage (J–V) curve of the device. (b) EQE spectra of devices at optimized conditions. (c) J_{ph} *versus* V_{eff} and (d) light intensity (P) dependence of J_{sc} for the optimized FCO-2F based devices.

miscibility of donors and acceptors with a small root-mean-square surface roughness value of 1.82 nm, which is similar to that of the F-H based film (1.69 nm shown in Fig. S4, ESI†). Furthermore, as shown in the TEM image in Fig. 5b, the PM6:FCO-2F film has obvious fiber-like interpenetrating network nanostructures, indicating an optimal morphology of the donor and acceptor mixture as that for F-H. To have a further understanding of molecular packing and morphology in the FCO-2F based active layer, the grazing-incidence wide-angle X-ray scattering (GIWAXS) analysis was carried out. As shown in Fig. S5 in the ESI,† in the pristine film, FCO-2F shows a weak differentiation peak, while after TA, the differentiation peak becomes stronger. These indicate that there is increased ordered packing after TA. In the out-of-plane (OOP) direction, FCO-2F shows a pronounced π–π stacking diffraction peak (010) at 1.93 $Å^{-1}$ with the π–π stacking distance of 3.25 Å. In the in-plane (IP) direction, an obvious laminar packing diffraction peak (100) at 0.36 $Å^{-1}$ could be seen. These results indicate that the FCO-2F film prefers a face-on crystalline orientation. In the binary blending film of PM6:FCO-2F (Fig. 5c), a clear face-on diffraction peak is located at 1.88 $Å^{-1}$ in the OOP direction, corresponding to a π–π stacking distance of 3.33 Å. The crystal coherence length (CCL) for PM6:FCO-2F is calculated from the Scherrer equation (CCL = $2\pi k$/fwhm)[71] and has the value of 44.8 Å. The shorter π–π stacking distance and the face-on molecular orientation of the PM6:FCO-2F blend film are clearly in line with its much higher electron mobility.

Conclusions

In conclusion, an A–D–A small molecule acceptor FCO-2F with inserted oxygen in the backbone of F-H and a difluoro substituted end group was designed and synthesized. FCO-2F demonstrates a much red-shifted absorption with an absorption onset of 830 nm. By blending with polymer donor PM6, the OSC devices based on PM6:FCO-2F exhibit a PCE of 13.36%, one of the highest efficiencies for oxygen heterocycle-fused non-fullerene acceptors. A much improved J_{sc} of 20.90 mA cm^{-2} is achieved due to the red-shifted absorption, which is much higher than the J_{sc} of 15.81 mA cm^{-2} for F-H based devices. Considering the absorption spectrum of this kind of oxygen heterocycle-fused acceptor is still not red-shifted enough, more efforts should be put into the absorption modification to harvest more light and further improve the performance of OSCs.

Conflicts of interest

The authors declare no conflict of interest.

Acknowledgements

The authors gratefully acknowledge the financial support from MoST (2019YFA0705900, 2016YFA0200200), NSFC (21935007, 51773095 and 51873089) of China and 111 Project (B12015). The authors also thank beam line 1W1A (Beijing Synchrotron Radiation Laboratory Institute of High Energy Physics) for providing the beam time.

References

1 Z. Li, G. He, X. Wan, Y. Liu, J. Zhou, G. Long, Y. Zuo, M. Zhang and Y. Chen, Solution Processable Rhodanine-Based Small Molecule Organic Photovoltaic Cells with a Power Conversion Efficiency of 6.1%, *Adv. Energy Mater.*, 2012, **2**, 74–77.
2 G. Yu, J. Gao, J. C. Hummelen, F. Wudl and A. J. Heeger, Polymer Photovoltaic Cells: Enhanced Efficiencies via a Network of Internal Donor-Acceptor Heterojunctions, *Science*, 1995, **270**, 1789–1791.
3 F. C. Krebs, Fabrication and processing of polymer solar cells: A review of printing and coating techniques, *Sol. Energy Mater. Sol. Cells*, 2009, **93**, 394–412.
4 J. Yuan, Y. Zhang, L. Zhou, G. Zhang, H.-L. Yip, T.-K. Lau, X. Lu, C. Zhu, H. Peng, P. A. Johnson, M. Leclerc, Y. Cao, J. Ulanski, Y. Li and Y. Zou, Single-Junction Organic Solar Cell with over 15% Efficiency Using Fused-Ring Acceptor with Electron-Deficient Core, *Joule*, 2019, **3**, 1140–1151.
5 B. Fan, D. Zhang, M. Li, W. Zhong, Z. Zeng, L. Ying, F. Huang and Y. Cao, Achieving over 16% efficiency for single-junction organic solar cells, *Sci. China: Chem.*, 2019, **62**, 746–752.
6 Y. Cui, H. Yao, J. Zhang, T. Zhang, Y. Wang, L. Hong, K. Xian, B. Xu, S. Zhang, J. Peng, Z. Wei, F. Gao and J. Hou, Over 16% efficiency organic photovoltaic cells enabled by a chlorinated acceptor with increased open-circuit voltages, *Nat. Commun.*, 2019, **10**, 2515.
7 X. Xu, K. Feng, Z. Bi, W. Ma, G. Zhang and Q. Peng, Single-Junction Polymer Solar Cells with 16.35% Efficiency Enabled by a Platinum(II) Complexation Strategy, *Adv. Mater.*, 2019, **31**, 1901872.
8 K. Li, Y. Wu, Y. Tang, M. A. Pan, W. Ma, H. Fu, C. Zhan and J. Yao, Ternary Blended Fullerene-Free Polymer Solar Cells with 16.5% Efficiency Enabled with a Higher-LUMO-Level Acceptor to Improve Film Morphology, *Adv. Energy Mater.*, 2019, **9**, 1901728.
9 Q. An, X. Ma, J. Gao and F. Zhang, Solvent additive-free ternary polymer solar cells with 16.27% efficiency, *Sci. Bull.*, 2019, **64**, 504–506.
10 K. Jiang, Q. Wei, J. Y. L. Lai, Z. Peng, H. K. Kim, J. Yuan, L. Ye, H. Ade, Y. Zou and H. Yan, Alkyl Chain Tuning of Small Molecule Acceptors for Efficient Organic Solar Cells, *Joule*, 2019, **3**, 3020–3033.
11 J. Xiong, K. Jin, Y. Jiang, J. Qin, T. Wang, J. Liu, Q. Liu, H. Peng, X. Li, A. Sun, X. Meng, L. Zhang, L. Liu, W. Li, Z. Fang, X. Jia, Z. Xiao, Y. Feng, X. Zhang, K. Sun, S. Yang, S. Shi and L. Ding, Thiolactone copolymer donor gifts organic solar cells a 16.72% efficiency, *Sci. Bull.*, 2019, **64**, 1573–1576.
12 L. Hong, H. Yao, Z. Wu, Y. Cui, T. Zhang, Y. Xu, R. Yu, Q. Liao, B. Gao, K. Xian, H. Y. Woo, Z. Ge and J. Hou,

Eco-Compatible Solvent-Processed Organic Photovoltaic Cells with Over 16% Efficiency, *Adv. Mater.*, 2019, **31**, 1903441.

13 Q. Liu, Y. Jiang, K. Jin, J. Qin, J. Xu, W. Li, J. Xiong, J. Liu, Z. Xiao, K. Sun, S. Yang, X. Zhang and L. Ding, 18% efficiency organic solar cells, *Sci. Bull.*, 2020, **65**, 272–275.

14 Q. An, J. Wang, W. Gao, X. Ma, Z. Hu, J. Gao, C. Xu, M. Hao, X. Zhang, C. Yang and F. Zhang, Alloy-like ternary polymer solar cells with over 17.2% efficiency, *Sci. Bull.*, 2020, **65**, 538–545, DOI: 10.1016/j.scib.2020.01.012.

15 L. Zhan, S. Li, T.-K. Lau, Y. Cui, X. Lu, M. Shi, C.-Z. Li, H. Li, J. Hou and H. Chen, Over 17% efficiency ternary organic solar cells enabled by two non-fullerene acceptors working in an alloy-like model, *Energy Environ. Sci.*, 2020, **13**, 635–645.

16 L. Meng, Y. Zhang, X. Wan, C. Li, X. Zhang, Y. Wang, X. Ke, Z. Xiao, L. Ding, R. Xia, H.-L. Yip, Y. Cao and Y. Chen, Organic and solution-processed tandem solar cells with 17.3% efficiency, *Science*, 2018, **361**, 1094–1098.

17 Z. Zhou, W. Liu, G. Zhou, M. Zhang, D. Qian, J. Zhang, S. Chen, S. Xu, C. Yang, F. Gao, H. Zhu, F. Liu and X. Zhu, Subtle Molecular Tailoring Induces Significant Morphology Optimization Enabling over 16% Efficiency Organic Solar Cells with Efficient Charge Generation, *Adv. Mater.*, 2019, **32**, 1906324.

18 C. Sun, S. Qin, R. Wang, S. Chen, F. Pan, B. Qiu, Z. Shang, L. Meng, C. Zhang, M. Xiao, C. Yang and Y. Li, High Efficiency Polymer Solar Cells with Efficient Hole Transfer at Zero Highest Occupied Molecular Orbital Offset between Methylated Polymer Donor and Brominated Acceptor, *J. Am. Chem. Soc.*, 2020, **142**, 1465–1474.

19 Y. Xu, H. Yao and J. Hou, Recent Advances in Fullerene-free Polymer Solar Cells: Materials and Devices, *Chin. J. Chem.*, 2019, **37**, 207–215.

20 J. Zhang, H. S. Tan, X. Guo, A. Facchetti and H. Yan, Material insights and challenges for non-fullerene organic solar cells based on small molecular acceptors, *Nat. Energy*, 2018, **3**, 720–731.

21 P. Cheng, G. Li, X. Zhan and Y. Yang, Next-generation organic photovoltaics based on non-fullerene acceptors, *Nat. Photonics*, 2018, **12**, 131–142.

22 W. Zhao, S. Li, H. Yao, S. Zhang, Y. Zhang, B. Yang and J. Hou, Molecular Optimization Enables over 13% Efficiency in Organic Solar Cells, *J. Am. Chem. Soc.*, 2017, **139**, 7148–7151.

23 Z. Fei, F. D. Eisner, X. Jiao, M. Azzouzi, J. A. Rohr, Y. Han, M. Shahid, A. S. R. Chesman, C. D. Easton, C. R. McNeill, T. D. Anthopoulos, J. Nelson and M. Heeney, An Alkylated Indacenodithieno[3,2-*b*]thiophene-Based Nonfullerene Acceptor with High Crystallinity Exhibiting Single Junction Solar Cell Efficiencies Greater than 13% with Low Voltage Losses, *Adv. Mater.*, 2018, **30**, 1705209.

24 J. Sun, X. Ma, Z. Zhang, J. Yu, J. Zhou, X. Yin, L. Yang, R. Geng, R. Zhu, F. Zhang and W. Tang, Dithieno[3,2-*b*:2′,3′-*d*]pyrrol Fused Nonfullerene Acceptors Enabling Over 13% Efficiency for Organic Solar Cells, *Adv. Mater.*, 2018, **30**, 1707150.

25 D. He, F. Zhao, J. Xin, J. J. Rech, Z. Wei, W. Ma, W. You, B. Li, L. Jiang, Y. Li and C. Wang, A Fused Ring Electron Acceptor with Decacyclic Core Enables over 13.5% Efficiency for Organic Solar Cells, *Adv. Energy Mater.*, 2018, **8**, 1802050.

26 W. Liu, J. Zhang, Z. Zhou, D. Zhang, Y. Zhang, S. Xu and X. Zhu, Design of a New Fused-Ring Electron Acceptor with Excellent Compatibility to Wide-Bandgap Polymer Donors for High-Performance Organic Photovoltaics, *Adv. Mater.*, 2018, **30**, 1800403.

27 C. Huang, X. Liao, K. Gao, L. Zuo, F. Lin, X. Shi, C.-Z. Li, H. Liu, X. Li, F. Liu, Y. Chen, H. Chen and A. K. Y. Jen, Highly Efficient Organic Solar Cells Based on S,N-Heteroacene Non-Fullerene Acceptors, *Chem. Mater.*, 2018, **30**, 5429–5434.

28 Y. Chen, X. Wan and G. Long, High Performance Photovoltaic Applications Using Solution-Processed Small Molecules, *Acc. Chem. Res.*, 2013, **46**, 2645–2655.

29 Y. Liu, X. Wan, B. Yin, J. Zhou, G. Long, S. Yin and Y. Chen, Efficient solution processed bulk-heterojunction solar cells based a donor–acceptor oligothiophene, *J. Mater. Chem.*, 2010, **20**, 2464.

30 Q. Jiang, Y. Zhao, X. Zhang, X. Yang, Y. Chen, Z. Chu, Q. Ye, X. Li, Z. Yin and J. You, Surface passivation of perovskite film for efficient solar cells, *Nat. Photonics*, 2019, **13**, 460–466.

31 X.-X. Gao, D.-J. Xue, D. Gao, Q. Han, Q.-Q. Ge, J.-Y. Ma, J. Ding, W. Zhang, B. Zhang, Y. Feng, G. Yu and J.-S. Hu, High-Mobility Hydrophobic Conjugated Polymer as Effective Interlayer for Air-Stable Efficient Perovskite Solar Cells, *Sol. RRL*, 2019, **3**, 1800232.

32 J. Hou, O. Inganäs, R. H. Friend and F. Gao, Organic solar cells based on non-fullerene acceptors, *Nat. Mater.*, 2018, **17**, 119–128.

33 X. Shi, X. Liao, K. Gao, L. Zuo, J. Chen, J. Zhao, F. Liu, Y. Chen and A. K. Y. Jen, An Electron Acceptor with Broad Visible-NIR Absorption and Unique Solid State Packing for As-Cast High Performance Binary Organic Solar Cells, *Adv. Funct. Mater.*, 2018, **28**, 1802324.

34 H. Yao, Y. Cui, R. Yu, B. Gao, H. Zhang and J. Hou, Design, Synthesis, and Photovoltaic Characterization of a Small Molecular Acceptor with an Ultra-Narrow Band Gap, *Angew. Chem., Int. Ed.*, 2017, **56**, 3045–3049.

35 Z. Xiao, X. Jia, D. Li, S. Wang, X. Geng, F. Liu, J. Chen, S. Yang, T. P. Russell and L. Ding, 26 mA cm^{-2} J_{sc} from organic solar cells with a low-bandgap nonfullerene acceptor, *Sci. Bull.*, 2017, **62**, 1494–1496.

36 W. Ni, X. Wan, M. Li, Y. Wang and Y. Chen, A–D–A small molecules for solution-processed organic photovoltaic cells, *Chem. Commun.*, 2015, **51**, 4936–4950.

37 Y. Lin, J. Wang, Z. G. Zhang, H. Bai, Y. Li, D. Zhu and X. Zhan, An electron acceptor challenging fullerenes for efficient polymer solar cells, *Adv. Mater.*, 2015, **27**, 1170–1174.

38 S. Dai, F. Zhao, Q. Zhang, T. K. Lau, T. Li, K. Liu, Q. Ling, C. Wang, X. Lu, W. You and X. Zhan, Fused Nonacyclic Electron Acceptors for Efficient Polymer Solar Cells, *J. Am. Chem. Soc.*, 2017, **139**, 1336–1343.

39 Y.-Q.-Q. Yi, H. Feng, M. Chang, H. Zhang, X. Wan, C. Li and Y. Chen, New small-molecule acceptors based on hexacyclic naphthalene(cyclopentadithiophene) for efficient non-fullerene organic solar cells, *J. Mater. Chem. A*, 2017, **5**, 17204–17210.

40 H. Feng, Y. Q. Q. Yi, X. Ke, J. Yan, Y. Zhang, X. Wan, C. Li, N. Zheng, Z. Xie and Y. Chen, New Anthracene-Fused Nonfullerene Acceptors for High-Efficiency Organic Solar Cells: Energy Level Modulations Enabling Match of Donor and Acceptor, *Adv. Energy Mater.*, 2019, **9**, 1803541.

41 Y. Sun, H.-H. Gao, Y.-Q.-Q. Yi, X. Wan, H. Feng, X. Ke, Y. Zhang, J. Yan, C. Li and Y. Chen, Fluorination-modulated end units for high-performance non-fullerene acceptors based organic solar cells, *Sci. China Mater.*, 2019, **62**, 1210–1217.

42 J. Wang, J. Zhang, Y. Xiao, T. Xiao, R. Zhu, C. Yan, Y. Fu, G. Lu, X. Lu, S. R. Marder and X. Zhan, Effect of Isomerization on High-Performance Nonfullerene Electron Acceptors, *J. Am. Chem. Soc.*, 2018, **140**, 9140–9147.

43 X. Shi, J. Chen, K. Gao, L. Zuo, Z. Yao, F. Liu, J. Tang and A. K. Y. Jen, Terthieno[3,2-b]Thiophene (6T) Based Low Bandgap Fused-Ring Electron Acceptor for Highly Efficient Solar Cells with a High Short-Circuit Current Density and Low Open-Circuit Voltage Loss, *Adv. Energy Mater.*, 2018, **8**, 1702831.

44 T. Li, S. Dai, Z. Ke, L. Yang, J. Wang, C. Yan, W. Ma and X. Zhan, Fused Tris(thienothiophene)-Based Electron Acceptor with Strong Near-Infrared Absorption for High-Performance As-Cast Solar Cells, *Adv. Mater.*, 2018, **30**, 1705969.

45 H. Yao, Y. Chen, Y. Qin, R. Yu, Y. Cui, B. Yang, S. Li, K. Zhang and J. Hou, Design and Synthesis of a Low Bandgap Small Molecule Acceptor for Efficient Polymer Solar Cells, *Adv. Mater.*, 2016, **28**, 8283–8287.

46 Y. Liu, Z. Zhang, S. Feng, M. Li, L. Wu, R. Hou, X. Xu, X. Chen and Z. Bo, Exploiting Noncovalently Conformational Locking as a Design Strategy for High Performance Fused-Ring Electron Acceptor Used in Polymer Solar Cells, *J. Am. Chem. Soc.*, 2017, **139**, 3356–3359.

47 Y. Liu, C. e. Zhang, D. Hao, Z. Zhang, L. Wu, M. Li, S. Feng, X. Xu, F. Liu, X. Chen and Z. Bo, Enhancing the Performance of Organic Solar Cells by Hierarchically Supramolecular Self-Assembly of Fused-Ring Electron Acceptors, *Chem. Mater.*, 2018, **30**, 4307–4312.

48 D. Liu, B. Kan, X. Ke, N. Zheng, Z. Xie, D. Lu and Y. Liu, Extended Conjugation Length of Nonfullerene Acceptors with Improved Planarity via Noncovalent Interactions for High-Performance Organic Solar Cells, *Adv. Energy Mater.*, 2018, **8**, 1801618.

49 D. Liu, T. Wang, X. Ke, N. Zheng, Z. Chang, Z. Xie and Y. Liu, Ultra-narrow bandgap non-fullerene acceptors for organic solar cells with low energy loss, *Mater. Chem. Front.*, 2019, **3**, 2157–2163.

50 Z. Xiao, X. Jia and L. Ding, Ternary organic solar cells offer 14% power conversion efficiency, *Sci. Bull.*, 2017, **62**, 1562–1564.

51 X. Li, H. Huang, Z. Peng, C. Sun, D. Yang, J. Zhou, A. Liebman-Pelaez, C. Zhu, Z.-G. Zhang, Z. Zhang, Z. Xie, H. Ade and Y. Li, Effects of fused-ring regiochemistry on the properties and photovoltaic performance of n-type organic semiconductor acceptors, *J. Mater. Chem. A*, 2018, **6**, 15933–15941.

52 Y. Zhou, M. Li, J. Song, Y. Liu, J. Zhang, L. Yang, Z. Zhang, Z. Bo and H. Wang, High efficiency small molecular acceptors based on novel O-functionalized ladder-type dipyran building block, *Nano Energy*, 2018, **45**, 10–20.

53 H. Wu, H. Fan, S. Xu, L. Ye, Y. Guo, Y. Yi, H. Ade and X. Zhu, Isomery-Dependent Miscibility Enables High-Performance All-Small-Molecule Solar Cells, *Small*, 2019, **15**, 1804271.

54 L. Dou, C.-C. Chen, K. Yoshimura, K. Ohya, W.-H. Chang, J. Gao, Y. Liu, E. Richard and Y. Yang, Synthesis of 5H-Dithieno[3,2-*b*:2′,3′-*d*]pyran as an Electron-Rich Building Block for Donor–Acceptor Type Low-Bandgap Polymers, *Macromolecules*, 2013, **46**, 3384–3390.

55 L. Yang, M. Li, J. Song, Y. Zhou, Z. Bo and H. Wang, Molecular Consideration for Small Molecular Acceptors Based on Ladder-Type Dipyran: Influences of O-Functionalization and π-Bridges, *Adv. Funct. Mater.*, 2018, **28**, 1705927.

56 Z. Luo, H. Bin, T. Liu, Z. G. Zhang, Y. Yang, C. Zhong, B. Qiu, G. Li, W. Gao, D. Xie, K. Wu, Y. Sun, F. Liu, Y. Li and C. Yang, Fine-Tuning of Molecular Packing and Energy Level through Methyl Substitution Enabling Excellent Small Molecule Acceptors for Nonfullerene Polymer Solar Cells with Efficiency up to 12.54%, *Adv. Mater.*, 2018, **30**, 1706124.

57 W. Gao, T. Liu, R. Ming, Z. Luo, K. Wu, L. Zhang, J. Xin, D. Xie, G. Zhang, W. Ma, H. Yan and C. Yang, Near-Infrared Small Molecule Acceptor Enabled High-Performance Non-fullerene Polymer Solar Cells with Over 13% Efficiency, *Adv. Funct. Mater.*, 2018, **28**, 1803128.

58 Y. Cui, H. Yao, B. Gao, Y. Qin, S. Zhang, B. Yang, C. He, B. Xu and J. Hou, Fine Tuned Photoactive and Interconnection Layers for Achieving over 13% Efficiency in a Fullerene-free Tandem Organic Solar Cell, *J. Am. Chem. Soc.*, 2017, **139**, 7302–7309.

59 H. Yao, L. Ye, J. Hou, B. Jang, G. Han, Y. Cui, G. M. Su, C. Wang, B. Gao, R. Yu, H. Zhang, Y. Yi, H. Y. Woo, H. Ade and J. Hou, Achieving Highly Efficient Nonfullerene Organic Solar Cells with Improved Intermolecular Interaction and Open-Circuit Voltage, *Adv. Mater.*, 2017, **29**, 1700254.

60 J. Zhang, Y. Li, H. Hu, G. Zhang, H. Ade and H. Yan, Chlorinated Thiophene End Groups for Highly Crystalline Alkylated Non-Fullerene Acceptors toward Efficient Organic Solar Cells, *Chem. Mater.*, 2019, **31**, 6672–6676.

61 H. Feng, N. Qiu, X. Wang, Y. Wang, B. Kan, X. Wan, M. Zhang, A. Xia, C. Li, F. Liu, H. Zhang and Y. Chen, An A–D–A Type Small-Molecule Electron Acceptor with End-Extended Conjugation for High Performance Organic Solar Cells, *Chem. Mater.*, 2017, **29**, 7908–7917.

62 G. He, Z. Li, X. Wan, J. Zhou, G. Long, S. Zhang, M. Zhang and Y. Chen, Efficient small molecule bulk heterojunction solar cells with high fill factors via introduction of π-stacking moieties as end group, *J. Mater. Chem. A*, 2013, **1**, 1801–1809.

63 M. Li, Y. Liu, W. Ni, F. Liu, H. Feng, Y. Zhang, T. Liu, H. Zhang, X. Wan, B. Kan, Q. Zhang, T. P. Russell and Y. Chen, A simple small molecule as an acceptor for fullerene-free organic solar cells with efficiency near 8%, *J. Mater. Chem. A*, 2016, **4**, 10409–10413.

64 Y. Li, J. D. Lin, X. Che, Y. Qu, F. Liu, L. S. Liao and S. R. Forrest, High Efficiency Near-Infrared and Semitransparent Non-Fullerene Acceptor Organic Photovoltaic Cells, *J. Am. Chem. Soc.*, 2017, **139**, 17114–17119.

65 F. Yang, C. Li, W. Lai, A. Zhang, H. Huang and W. Li, Halogenated conjugated molecules for ambipolar field-effect transistors and non-fullerene organic solar cells, *Mater. Chem. Front.*, 2017, **1**, 1389–1395.

66 N. Qiu, H. Zhang, X. Wan, C. Li, X. Ke, H. Feng, B. Kan, H. Zhang, Q. Zhang, Y. Lu and Y. Chen, A New Nonfullerene Electron Acceptor with a Ladder Type Backbone for High-Performance Organic Solar Cells, *Adv. Mater.*, 2017, **29**, 1604964.

67 W. Shockley and H. J. Queisser, Detailed Balance Limit of Efficiency of p–n Junction Solar Cells, *J. Appl. Phys.*, 1961, **32**, 510–519.

68 M. J. Frisch, G. W. Trucks, H. B. Schlegel, G. E. Scuseria, M. A. Robb, J. R. Cheeseman, G. Scalmani, V. Barone, G. A. Petersson, H. Nakatsuji, X. Li, M. Caricato, A. V. Marenich, J. Bloino, B. G. Janesko, R. Gomperts, B. Mennucci, H. P. Hratchian, J. V. Ortiz, A. F. Izmaylov, J. L. Sonnenberg, F. Ding Williams, F. Lipparini, F. Egidi, J. Goings, B. Peng, A. Petrone, T. Henderson, D. Ranasinghe, V. G. Zakrzewski, J. Gao, N. Rega, G. Zheng, W. Liang, M. Hada, M. Ehara, K. Toyota, R. Fukuda, J. Hasegawa, M. Ishida, T. Nakajima, Y. Honda, O. Kitao, H. Nakai, T. Vreven, K. Throssell, J. A. Montgomery, Jr., J. E. Peralta, F. Ogliaro, M. J. Bearpark, J. J. Heyd, E. N. Brothers, K. N. Kudin, V. N. Staroverov, T. A. Keith, R. Kobayashi, J. Normand, K. Raghavachari, A. P. Rendell, J. C. Burant, S. S. Iyengar, J. Tomasi, M. Cossi, J. M. Millam, M. Klene, C. Adamo, R. Cammi, J. W. Ochterski, R. L. Martin, K. Morokuma, O. Farkas, J. B. Foresman and D. J. Fox, *Gaussian 16, Revision A.03*, Gaussian, Inc., Wallingford CT, 2016.

69 C. M. Proctor, M. Kuik and T.-Q. Nguyen, Charge carrier recombination in organic solar cells, *Prog. Polym. Sci.*, 2013, **38**, 1941–1960.

70 Y. Wang, Y. Zhang, N. Qiu, H. Feng, H. Gao, B. Kan, Y. Ma, C. Li, X. Wan and Y. Chen, A Halogenation Strategy for over 12% Efficiency Nonfullerene Organic Solar Cells, *Adv. Energy Mater.*, 2018, **8**, 1702870.

71 D. M. Smilgies, Scherrer grain-size analysis adapted to grazing-incidence scattering with area detectors, *J. Appl. Crystallogr.*, 2009, **42**, 1030–1034.